



**HAL**  
open science

# Lineage Tracing Reveals the Dynamic Contribution of Pericytes to the Blood Vessel Remodeling in Pulmonary Hypertension

Jennifer Bordenave, Ly Tu, Nihel Berrebeh, Raphaël Thuillet, Amélie Cumont, Benjamin Le Vely, Elie Fadel, Sophie Nadaud, Laurent Savale, Marc Humbert, et al.

► **To cite this version:**

Jennifer Bordenave, Ly Tu, Nihel Berrebeh, Raphaël Thuillet, Amélie Cumont, et al.. Lineage Tracing Reveals the Dynamic Contribution of Pericytes to the Blood Vessel Remodeling in Pulmonary Hypertension. *Arteriosclerosis, Thrombosis, and Vascular Biology*, 2020, 40 (3), pp.766-782. 10.1161/ATVBAHA.119.313715 . inserm-02454982v2

**HAL Id: inserm-02454982**

**<https://inserm.hal.science/inserm-02454982v2>**

Submitted on 19 May 2020

**HAL** is a multi-disciplinary open access archive for the deposit and dissemination of scientific research documents, whether they are published or not. The documents may come from teaching and research institutions in France or abroad, or from public or private research centers.

L'archive ouverte pluridisciplinaire **HAL**, est destinée au dépôt et à la diffusion de documents scientifiques de niveau recherche, publiés ou non, émanant des établissements d'enseignement et de recherche français ou étrangers, des laboratoires publics ou privés.

# Lineage Tracing Reveals the Dynamic Contribution of Pericytes To the Blood Vessel Remodeling In Pulmonary Hypertension

**Running title:** *Bordenave et al.; Pericytes in the Pulmonary Blood Vessel Remodeling*

Jennifer Bordenave (PhD)<sup>1,2</sup>, Ly Tu (PhD)<sup>1,2</sup>, Nihel Berrebeh (PharmD, MSc)<sup>1,2</sup>, Raphaël Thuillet (MSc)<sup>1,2</sup>, Amélie Cumont (BSc)<sup>1,2</sup>, Benjamin Le Vely (MSc)<sup>1,2</sup>, Elie Fadel (MD, PhD)<sup>1,2</sup>, Sophie Nadaud (PhD)<sup>4</sup>, Laurent Savale (MD, PhD)<sup>1,2,3</sup>, Marc Humbert (MD, PhD)<sup>1,2,3</sup>, Alice Huertas (MD, PhD)<sup>1,2,3</sup>, Christophe Guignabert (PhD)<sup>1,2</sup>

<sup>1</sup> INSERM UMR\_S 999, Hôpital Marie Lannelongue, 92350 Le Plessis-Robinson, France ;

<sup>2</sup> Faculté de Médecine, Université Paris-Sud, Université Paris-Saclay, 94270 Le Kremlin-Bicêtre, France ;

<sup>3</sup> Service de Pneumologie, AP-HP, Centre de Référence de l'Hypertension Pulmonaire Sévère, Hôpital Bicêtre, 94270 Le Kremlin-Bicêtre, France ;

<sup>4</sup> Institute of Cardiometabolism and Nutrition (ICAN), INSERM UMR\_S 1166, Hôpital la Pitié Salpêtrière, 75013 Paris, France.

## **Address for correspondence:**

Christophe Guignabert, PhD

INSERM UMR\_S 999

Hôpital Marie Lannelongue

133, Avenue de la Résistance

92350 Le Plessis-Robinson, France.

Tel: +33-1-40948833

Fax: +33-1-40942522

Email: [christophe.guignabert@inserm.fr](mailto:christophe.guignabert@inserm.fr)

## Abstract:

**Objective:** Excessive accumulation of resident cells within the pulmonary vascular wall represents the hallmark feature of the remodeling occurring in pulmonary arterial hypertension (PAH). Furthermore, we have previously demonstrated that pulmonary arterioles are excessively covered by pericytes in PAH, but this process is not fully understood. The aim of our study was to investigate the dynamic contribution of pericytes in PAH vascular remodeling.

**Approach and Results:** In this study, we performed *in situ*, *in vivo* and *in vitro* experiments. We isolated primary cultures of human pericytes from controls and PAH lung specimens then performed functional studies (cell migration, proliferation and differentiation). In addition, to follow up pericyte number and fate, a genetic fate mapping approach was used with a *NG2CreER<sup>TM</sup>;mT/mG* transgenic mice in a model of pulmonary arteriole muscularization occurring during chronic hypoxia. We identified phenotypic and functional abnormalities of PAH pericytes *in vitro*, as they overexpress CXCR7 and TGF $\beta$ RII and, thereby, display a higher capacity to migrate, proliferate and differentiate into smooth muscle-like cells than controls. In an *in vivo* model of chronic hypoxia, we found an early increase in pericyte number in a CXCL12-dependent manner whereas later, from day 7, activation of the canonical TGF- $\beta$  signaling pathway induces pericytes to differentiate into smooth muscle-like cells.

**Conclusions:** Our findings reveal a pivotal role of pulmonary pericytes in PAH and identify CXCR7 and TGF $\beta$ RII as two intrinsic abnormalities in these resident progenitor vascular cells that foster the onset and maintenance of PAH structural changes in blood lung vessels.

**Keywords:** *pulmonary hypertension, vascular remodeling, mesenchymal stem cells, pericyte, mural cells, lineage tracing*

## HIGHLIGHTS

- We identify phenotypic and functional abnormalities of pulmonary pericytes in idiopathic PAH with pathogenetic significance.
- We show that pulmonary pericytes from idiopathic PAH patients overexpress CXCR-7 and TGF $\beta$ RII, underlying their excessive proliferation/migration capacities and myogenic potentials, respectively.
- We provide multiple lines of evidence showing that pericytes dynamically contribute to the pulmonary vascular remodelling induced by chronic hypoxia.
- In chronic hypoxia, CXCL12/CXCR4/CXCR7 axis is required for pericyte accumulation in lungs and TGF $\beta$ /TGF $\beta$ RII axis plays a central role in their differentiation into contractile cells.

## INTRODUCTION

Inappropriate and sustained remodeling of blood lung vessels causes significant hemodynamic changes and is a major contributor to morbidity, disability and mortality in patients with pulmonary arterial hypertension (PAH) <sup>1</sup>. Treatment options are limited, and in severe cases, chronic right heart failure and premature death arise. Excessive accumulation of resident cells within the blood vessel wall represents hallmark feature of the blood vessel remodeling in PAH, but the underlying cell biological processes are not well defined <sup>2</sup>.

Pericytes (PCs) are found around pre-capillary arteries, capillaries, and post-capillary venules <sup>3</sup>. They occupy a strategic position at the interface between circulating blood and interstitial space, and at close proximity to endothelial (ECs) and smooth muscle cells (SMCs). PCs are central regulators of vascular development, stabilization, maturation, and remodeling, modulating: 1) EC growth, proliferation, differentiation and migration; 2) SMC contraction and capillary blood flow; 3) immune cell functions <sup>4-6</sup>. PCs also possess a multi-lineage differentiation potential. Importantly, we have recently reported excessive PC coverage in pulmonary arterioles in experimental and human PAH (a 2- to 3-fold increase), a phenomenon that contributes to vascular remodeling as a source of SMC-like cells <sup>7</sup>. However, the underlying mechanisms are still not elucidated. In particular, we do not know whether pulmonary PCs are phenotypically and functionally altered in PAH, and which dynamic role PCs play in pulmonary vascular remodeling.

In the current study, we identify that pulmonary PCs derived from patients with idiopathic PAH (iPAH) are phenotypically and functionally altered and delineate mechanisms underlying their expansion and dynamic contribution to the accumulation of contractile cells in blood vessel walls. Our findings indicate that PC-specific up-regulations of CXC chemokine receptor (CXCR)-7 and transforming growth factor (TGF)- $\beta$  receptor RII in PAH patients are critical for their excessive proliferation/ migration capacities and myogenic potentials, respectively. We also provide evidence that the neural glial antigen (NG)2-lineage expands in lungs of mice chronically exposed to hypoxia, a phenomenon abolished with CXC chemokine ligand (CXCL)-12 neutralization, and gives rise to  $\alpha$ -SMA positive cells that muscularize distal arterioles *in vivo*.

## METHODS

The data that support the findings of this study are available from the corresponding author upon reasonable request. The detailed description of the reagents and resources can be found in the Table S1.

### **Experimental Model and Subject Details:**

**Animals:** All animal work was in accordance with the animal ethics committee at University Paris-Sud, Le Plessis-Robinson, France (n°01176.01). Mice were housed in a pathogen-free barrier facility, under 14-hour light / 10-hour dark cycle and temperature-controlled environment with standard diet and water *ad libitum*. *B6.Cg-Tg(Cspg4-cre/Esr1\*)BAkik/J* (also known as *NG2CreER<sup>TM</sup>*) and *Gt(ROSA)26Sor<sup>tm4(ACTB-tdTomato,-EGFP)Luo/J</sup>* (also known as *mT/mG*) mice were purchased from The Jackson Laboratory. *NG2CreER<sup>TM</sup>* and *mT/mG* mice were crossed to generate *NG2CreER<sup>TM</sup>;mT/mG* mice. Both male and female adult mice (8-week-old mice) were used. Since no statistically significant sex-related differences were observed, individual data from males and female were pooled together. All animals were maintained on a *C57BL/6J* background. All animals were not involved in any previous procedure.

**Isolation, and culture of primary Human lung pericytes:** All experimental studies using human samples comply with the Declaration of Helsinki and were approved by the local ethics committee (*Comité de Protection des Personnes [CPP] Ile-de-France VII*). All patients gave informed consent before the study. Detailed demographic and clinical characteristics are shown in Supplemental

Table S2. Primary Human lung PCs were isolated from human lung specimens using an anti-3G5 antibody and anti-IgM magnetic beads on lung tissue fragment digested by collagenase type I<sup>7</sup>. Pulmonary PCs were cultured in Pericyte Medium (#1201 containing supplements; ScienCell, Carlsbad, CA) (complete medium) and are strongly positive for NG2 and PDGF receptor- $\beta$  and negative for  $\alpha$ -SMA, calponin and SMMHC. Cells were routinely tested for mycoplasma and used at early passages  $\leq 4$ .

### **Animal procedure**

Tamoxifen was resuspended in corn oil at 10 mg/mL and *NG2CreER<sup>TM</sup>;mT/mG* adult mice were intraperitoneally injected with 1 mg for 5 consecutive days (induction). Seven days post tamoxifen treatment, mice were chronically exposed to hypoxia (10% FiO<sub>2</sub>) or maintained in room air (21% FiO<sub>2</sub>). Chalcone 4 was resuspended in a solution of sodium carboxymethyl cellulose (CMC) and a group of *NG2CreER<sup>TM</sup>;mT/mG* adult mice injected with tamoxifen was intraperitoneally injected with vehicle or chalcone 4 at a dose of 100mg/kg/day. At the end of these protocols, pulmonary hemodynamic parameters were measured blindly in unventilated anesthetized mice as previously described<sup>7-10</sup>. Briefly, RVSP and heart rate were determined in unventilated mice under isoflurane anesthesia (1.5-2.5%, 2L O<sub>2</sub>/min.) using a closed chest technique, by introducing a catheter (1.4 F catheter, Millar Instruments Inc, Houston, TX) into the jugular vein and directing it to the right ventricle. After all the hemodynamic assessments were completed, blood was collected by direct cardiac puncture and sacrificed by exsanguinations. The heart and lungs were then removed *en bloc* and right ventricular hypertrophy (RVH) was determined by the Fulton index measurement (right ventricle/left ventricle plus septum RV/LV+S). The pulmonary circulation was flushed with 5mL of buffered saline at 37°C, and then the left lung was prepared for histological analyses and the right lung was quickly harvested, immediately snap-frozen in liquid nitrogen and kept at -80°C.

### **Immunofluorescent staining and microscopy**

Mouse lungs were fixed in 4% paraformaldehyde (PFA) for 10 min and then inflated by intratracheal administration of 2% low melting point agarose (Sigma-Aldrich) and incubated for 30 min at 4°C in ice-cold PBS. Then, agarose-filled lungs were immersed in a fixing solution (4:1 methanol:DMSO) at 4°C overnight, washed and stored in 100% methanol. The left lung lobe was isolated and sliced at a thickness of 150  $\mu$ m using a tissue slicer (LEICA VT1200S, Nanterre, France). Lung slices were blocked overnight with 5% bovine serum albumin in 0.5% triton X-100/PBS and then incubated with specific antibodies (1:50 MECA-32, 1:200 GFP, and 1:200  $\alpha$ -SMA) in 0.3% triton X-100/PBS for 3 days at 4°C, followed by corresponding secondary fluorescent-labeled antibodies overnight at 4°C (1:400; Thermo Fisher Scientific, Saint-Aubin, France). Immunofluorescent staining for 3G5 (1:50),  $\alpha$ -SMA (1:200), CXCR7 (1:200), and TGF- $\beta$ RII (1:200) were performed in lung paraffin sections as previously described<sup>7,9-11</sup>. Briefly, lung sections (5 $\mu$ m of thickness) were deparaffinized and incubated with the antigen retrieval buffer. Then, sections were saturated with blocking buffer and incubated overnight with specific antibodies, followed by addition of the corresponding secondary fluorescent-labelled antibodies (Thermo Fisher Scientific, Saint-Aubin, France). Nuclei were labelled using DAPI (Thermo Fisher Scientific). Mounting was performed using ProLong Gold antifade reagent (Thermo Fisher Scientific). All images were taken using a LSM700 confocal microscope (Zeiss, Marly-le-Roi, France).

### **Flow cytometry analysis and FACS**

Lung tissues were gently minced with scissors and digested with collagenase I (0.2%) and dispase (0.4%) in DMEM for 30 minutes in shaking water bath at 37°C. Digested tissue was then filtered through a 70  $\mu$ m filter and spin at 500 g at 4°C for 5 min. Flow cytometric analysis and sorting were performed using MACSQuant® Analyzer 10 Flow Cytometer (Miltenyi Biotec) and FlowJo software program (Tree Star, Inc). BD Cytofix/Cytoperm<sup>TM</sup> solution was used for the simultaneous fixation and permeabilization of cells prior to intracellular  $\alpha$ -SMA staining. Cell debris and erythrocytes were excluded from the analysis based on scatter signals, and Hoechst fluorescence.

### **Cell migration**

Cell migration was assessed using the *in vitro* wound-healing assay with the Ibidi Culture-Insert (Ibidi, Nanterre, France). Briefly, confluent monolayers were scratch wounded, and then incubated with 10% FCS for 8, 12 and 24 hours. Images were taken using a Zeiss Primo Vert inverted microscope (Zeiss, Marly-le-Roi, France). Cell migration was also assessed using a modified Boyden chamber chemotaxis system as described previously<sup>7, 12-14</sup>. Briefly, cells were seeded and allowed to migrate at 37°C for 6 hrs in presence of FCS, CXCL12, AMD3100, chalcone 4, or VUF 11207 at the indicated concentrations. Images were taken using KERN OBL-137 microscope (Kern, Balingen, Germany).

### **Cell proliferation**

Cell proliferation was measured by bromodeoxyuridine (BrdU) incorporation using the Delfia Cell proliferation kit (PerkinElmer, Waltham, MA, USA) and a time-resolved fluorometer EnVision Multilabel Reader (PerkinElmer, Waltham, MA, USA) as previously described<sup>7, 12-14</sup>. Briefly, cells were grown to 60% to 70% confluence at 37°C and exposed 24 hours to FCS, CXCL12, AMD3100, chalcone 4, or VUF 11207 at the indicated concentrations.

### **Cell differentiation**

The potential of PCs to differentiate into contractile cells was assessed by following expression of the contractile proteins SM22, calponin and  $\alpha$ -SMA, and the expression of collagen type I (Col1A) under serum deprivation (spontaneous differentiation) or after TGF- $\beta$  exposure (10ng/mL) during 48h. For serum deprivation, the Pericyte Medium (#1201-b from ScienCell without supplements) supplemented with 0.3% of fetal bovine serum (FBS) was used.

### **RNA isolation and RT-qPCR**

Total RNA was isolated from frozen lung using TRIZOL® protocol (Invitrogen, Carlsbad, CA), and RNeasy mini kit (Qiagen, Valencia, CA). Total RNA (2 $\mu$ g) was reverse-transcribed using Superscript II (Invitrogen, Carlsbad, CA) per manufacturer's instructions. RT-qPCR was performed on Step One Plus Real Time PCR machine (Applied Biosystems). Gene expression levels were quantified using pre-verified Assays-on-Demand TaqMan primer/probe sets (Applied Biosystems, Foster City, CA). The expression level of each gene was normalized to 18S ribosomal RNA using the comparative delta-CT method.

### **Western blot**

Cells/tissues were homogenized and sonicated in RIPA buffer containing protease and phosphatase inhibitors and 30  $\mu$ g of protein was used to detect SM22 (1:200), calponin (1:200),  $\alpha$ -SMA (1:200), Col1A (1:500), GFP (1:1000), NG2 (1:500), CXCR4 (1:200), CXCR7 (1:200), p-smad2/3 (1:200), TGF $\beta$ RII (1:200), TGF $\beta$ RI (1:200), GAPDH (1:5,000), and  $\beta$ -actin (1:50,000).

### **Image processing and quantification**

All images were composed, edited and modifications applied to the whole image using ZEN LSM (Carl Zeiss) and ImageJ (NIH) software. To measure the degree of co-localization in confocal images, co-localization coefficients were determined according to the method described by Manders *et al.*<sup>15</sup>.

### **Statistical Analyses**

All results are presented as mean  $\pm$  standard error of the mean (SEM). Statistical calculations were performed with GraphPad Prism 7 (GraphPad Software, Inc). The unpaired Student t test was used

after testing for normality and equal variance (Shapiro-Wilk test) to compare 2 groups. One-way ANOVA Tukey post hoc test were used to compare multiple groups if the data followed a normal distribution, otherwise nonparametric Kruskal-Wallis post hoc tests were used. Sample size is indicated in the figure legends. Results with p values of less than 0.05 were considered statistically significant.

## RESULTS

### **Pulmonary PCs are phenotypically and functionally altered in Human PAH**

To determine whether human pulmonary PCs from patients with idiopathic PAH exhibit an abnormal phenotype, primary PCs cultures were generated from lung specimens and used at early passages ( $\leq 4$ ) to evaluate their characteristics in terms of proliferation, migration and capacity to differentiate into contractile cells.

First, we isolated and characterized the 3G5 positive cells. Cultured PCs from control patients were strongly positive for NG2 and platelet-derived growth factor receptor (PDGFR)- $\beta$ , two well-known PC markers, mildly positive for SM22 and negative for  $\alpha$ -SMA, calponin, and smooth muscle myosin heavy chain (SMMHC) (**Figure 1A-B**). To better characterize primary human PC cultures, we used RT-qPCR and found absence of characteristic smooth muscle (**Figure 1C**), fibroblast (**Figure 1D**), and endothelial markers (**Figure S1**). In addition, they express several genes that are characteristics of multipotent cells such as CD73, CD90, c-kit, nestin, PEG3, RGS5 (**Figure 1E**). They also express high levels of S100 calcium-binding A4 (S100A4) (**Figure 1D**). Importantly, this extensive characterization has not revealed any differences between control and iPAH PCs.

We next endeavored to examine the cellular phenotype of pulmonary PCs derived from control and iPAH patients using *in vitro* functional studies. In the “scratch” wound closure assay, migration of iPAH PCs was more rapid by approximately 2- to 3-fold compared with control PCs (**Figure 2A**). Similarly, migration rates were increased for iPAH PCs placed on Boyden chambers as compared to controls cells (**Figure 2B**). We next extended these results using the bromodeoxyuridine (BrdU) incorporation assay to analyze and compare the proliferative capacity of control and iPAH PCs. The results showed that cultured PCs from iPAH patients proliferate 2 to 4 times faster than control PCs (**Figure 2C**). Finally, we examined expressions of different contractile proteins and compared their capacity to acquire a contractile phenotype under serum deprivation. No significant differences were observed between control and iPAH PCs in the complete medium, however iPAH PCs exhibited a higher myogenic potential than control PCs when they were serum deprived as reflected by the significant increases in SM22 and calponin, and the trend of increase in  $\alpha$ -SMA. In contrast, no difference was observed in col1A protein levels (**Figure 2D**). These results suggest the presence of intrinsic abnormalities in iPAH PCs that influence their cell behavior even when they are extracted from their pathological environment.

### **PCs dynamically contribute to the blood vessel remodeling in hypoxia-induced distal pulmonary arteriole muscularization**

To elucidate how PCs contribute to the remodeling of blood lung vessels, and if they give rise to  $\alpha$ -SMA positive cells to muscularize distal arterioles *in vivo*, we created the *NG2CreER<sup>TM</sup>;mT/mG* mouse line for the tracking of their lineage and fate during the pulmonary arteriole muscularization occurring with chronic hypoxia (**Figure 3A and S2**). Under physiological conditions, PCs are widely distributed through both lungs and different morphological features can be distinguished depending of their localization (**Figure 3B**). In precapillary vessels with a diameter  $> 70\mu\text{m}$ , PCs have a number of extensions and tend to wrap around the vessel. In the lung parenchyma, PCs are more elongated and display a multi-branched network, which is less prominent when they are localized on blood vessels.

Hypoxic exposure of *NG2CreER<sup>TM</sup>;mT/mG* mice injected with tamoxifen induced a rapid accumulation of green fluorescent protein (GFP) positive cells in mouse lungs, with a 3- and 5-fold increase after 2 and 4 days of hypoxia, respectively (**Figure 3C**). These findings suggest a rapid recruitment of PCs at these early time points following hypoxic exposure. To evaluate whether pulmonary PC acquire a contractile phenotype during the blood vessel remodeling in these mouse lungs, lung sections were stained with  $\alpha$ -SMA and quantified. The direct cell lineage tracing revealed a 8.5-, 8.1-, and 8.6-fold increase of  $\alpha$ -SMA positive PCs after 7, 14, and 21 days of hypoxia, indicating that PCs give rise to  $\alpha$ -SMA positive cells to muscularize distal pulmonary arterioles in mice chronically exposed to hypoxia (**Figure 3C**). Quantification of double positive cells for GFP and  $\alpha$ -SMA in mouse lungs by fluorescence-activated cell sorting (FACS) showed a significant increase in the percentage of GFP<sup>+</sup> cells (by 3.2-, 2.5-, 5.5-fold at Day-7, 14, and 21, respectively) and double positive  $\alpha$ -SMA<sup>+</sup> GFP<sup>+</sup> cells (by 2.1-, 1.7-, 3.3-fold at Day-7, 14, and 21, respectively) in mice chronically exposed to hypoxia when compared to control mice (**Figure 3D and S3**). Although less pronounced, we also noticed increase in numbers of GFP positive cells and changes in their morphology around larger blood vessels (> 70 $\mu$ m) (**Figure S4**).

As further validation, we fate mapped PCs during the sustained remodeling of blood lung vessels occurring with the combination of SU5416 (Sugen) and chronic hypoxia (SuHx) (**Figure 4A and S2B**). In this second mouse model, administration of SU5416 associated to chronic hypoxia is known to cause blood vessel rarefaction with pronounced accumulation of resident cells as well as components of the extracellular matrix within the blood vessel wall, which contribute to exaggerated PH in mice<sup>16</sup>. Consistent with our previous observations obtained in the chronic hypoxia mouse model, fate tracing also reveals that pulmonary PCs give rise to contractile cells in the SuHx mice (**Figure 4B-C**).

### **CXCL12 is required for the PC accumulation in lungs following hypoxic exposure**

Several studies suggest a central role for CXCL12 as a key signal to promote the migration of stem and progenitor cells to repair and regenerate damaged tissues, including in the blood vessel remodeling occurring in PAH<sup>17,18</sup>. In line with these notions, we found that the expression of CXCL12 was increased within the first 2 days of hypoxia exposure (**Figure 5A**), and remained elevated in mice studied on day 21 after exposure to hypoxia in presence or absence of SU5416 (**Figure 5A and S2C**). To determine the role of CXCL12 in PC accumulation observed in lungs following hypoxic exposure, we fate mapped PCs during hypoxia in randomized tamoxifen-injected *NG2CreER<sup>TM</sup>;mT/mG* mice treated with either vehicle or CXCL12 neutraligands chalcone 4 that prevent binding of CXCL12 to the receptors CXCR4 and CXCR7<sup>19,20</sup> (**Figure 5B**).

Immunofluorescence staining using lung vibratome sections indicated a reduction in numbers of GFP positive cells by 53.5% and 44% in mouse lungs of chalcone 4-treated mice exposed to 2 or 4 days of hypoxia compared to vehicle-treated mice, respectively (**Figure 5C**). Quantification of GFP positive cells in mouse lungs by FACS showed a reduction in GFP<sup>+</sup> cell numbers in mice treated with chalcone 4 when compared to vehicle-treated mice (**Figure 5D and S3**). Consistently, the increase in GFP and NG2 protein levels was reduced in lungs of tamoxifen-injected *NG2CreER<sup>TM</sup>;mT/mG* mice treated with chalcone 4 compared to vehicle-treated mice (**Figure 5E**). Together these results show that the chemokine CXCL12 is required for the early recruitment of PCs during the structural changes in blood lung vessels occurring with chronic hypoxia.

### **Up-regulation of CXCR7 underlies the excessive PC proliferation and migration in PAH**

To determine whether we could attribute the excessive proliferation/ migration capacities of PAH PCs to abnormality in the CXCL12 signaling, we exposed cultured PCs derived from healthy subjects and PAH patients to increasing doses of recombinant CXCL12. Quantification of their proliferative and migratory potentials showed that PAH PCs respond excessively to CXCL12 compared to control PCs (**Figure 6A-B**). Quantification of CXCR4 and CXCR7 protein levels, the two receptors for the chemokine CXCL12, showed that pulmonary PAH PCs exhibit up-regulation of the CXCR7 compared to control PCs (**Figure 6C**). Consistent with this observation, confocal

microscopic analyses and double labeling with CXCR7 (red) and the PC marker 3G5 (white) in lung specimens from patients with iPAH and control subjects (see Table S1) showed strong staining for CXCR7 in paraffin-embedded lungs of patients with iPAH when compared with control subjects (**Figure 6D**). Remarkably, CXCL12 neutralization with chalcone 4 attenuated the excessive proliferation/ migration capacities of PAH PCs (**Figure 6E-F**). In contrast, the conventional CXCR4 blockade with AMD3100 attenuated only the excessive PC migration, suggesting a role for CXCR7 in both PC proliferation and migration (**Figure 6E-F**). Consistent with this notion, the potent CXCR7 receptor agonist VUF 11207 (5 nM) increased the number of PAH PCs migrated through a polycarbonate membrane during six hours in response to 1% FCS (**Figure 6G**). Consistently, an increase in the rate of cell proliferation of control PCs exposed to 5 nM of VUF 11207 was also observed (**Figure 6H**). The overall results demonstrate that up-regulation of CXCR7 is required for the observed excessive PC proliferation and migration in PAH PCs. In addition, no effect of CXCL12 on the differentiation of PCs was noted (**Figure S6**).

### Up-regulation of TGF $\beta$ RII increased the PC ability to respond to TGF $\beta$ in PAH

Previous studies highlighted the importance of TGF- $\beta$  signaling in PC differentiation<sup>3,7,21</sup>, which prompted us to examine whether the ability of pulmonary PCs to respond to TGF- $\beta$  is altered or not in PAH cells. Exposure of control and PAH PCs to 10 ng/mL of recombinant TGF- $\beta$  for 48h resulted in a 2-fold increase in protein levels of  $\alpha$ -SMA and SM22 in PAH PCs compared to control PCs (**Figure 7A**). Phosphorylation of Smad2/3 was then analyzed by immunoblotting. Our results indicated that PAH PCs had approximately 2-fold to 3-fold higher induction of Smad2/3 phosphorylation in response to 10 ng/mL of recombinant TGF- $\beta$  when compared to control PCs (**Figure 7B**). To determine whether this exaggerated response to TGF- $\beta$  observed in PAH PCs was dependent on the receptor expressed, we next determined and compared the protein levels of TGF $\beta$ RI and TGF $\beta$ RII in control and PAH PCs. Quantification of the ratio of TGF $\beta$ RII:GAPDH revealed a 2-fold-increase in the TGF $\beta$ RII protein levels in PAH PCs compared to control PCs (**Figure 7C**). Consistently, confocal microscopic analyses and double labeling with TGF $\beta$ RII (red) and the PC marker 3G5 (green) in lung specimens from patients with iPAH and control subjects showed strong staining for TGF $\beta$ RII in pulmonary PCs in PAH when compared with control subjects (**Figure 7D**). No changes in TGF $\beta$ RI protein levels were noted between control and PAH PCs. These observations obtained in human lung specimens were replicated in tamoxifen-injected *NG2CreER<sup>TM</sup>;mT/mG* mice, with an significant increase in the expression of TGF $\beta$ RII in lungs of mice chronically exposed to hypoxia or in lungs of mice subjected to SU5416 and hypoxia (**Figure S7**). These results indicate that pulmonary PCs are more prone to respond to TGF- $\beta$  in PAH and therefore have greater myogenic potentials compared to healthy subjects.

## DISCUSSION

Pulmonary blood vessel remodeling is a dynamic process that occurs in response to alveolar hypoxia due to chronic lung diseases, prolonged exposure to high altitude or long-standing changes in hemodynamic conditions; however, it is also a well recognized complication of several pulmonary and cardiovascular diseases<sup>1</sup>. Thus, understanding the contribution of the different cell types involved in this process is central for the development of new therapeutic strategies to cure these cardiopulmonary vascular diseases and regenerate pulmonary blood vessels. In this context, PCs have recently gained new attention as central components of the pulmonary vessel wall, with important metabolic, signaling, and mechanical roles for blood vessel homeostasis and remodeling, but also because of their close interactions with the other resident pulmonary vascular cells and in particular with the endothelium. We have already reported that PCs accumulate either in the media or adventitia layers of remodeled pulmonary vessels in patients with idiopathic PAH, a phenomenon that is uniform and independent of vessel diameter, the presence of *BMPR2* mutations and of the degree and form of blood vessel remodeling<sup>7</sup>. Moreover, chronic exposure to hypoxia induces

blood vessel remodeling, a process that can be even more pronounced with a prior SU5416 administration<sup>7, 16, 22, 23</sup>. It is also known that CXCL12 and TGF- $\beta$  signaling are central pathways in pericyte-endothelial cell crosstalk and regulation<sup>3, 7, 17, 18, 21</sup>. In the current study, our objectives were to precise whether or not pulmonary PCs present intrinsic abnormalities in PAH and delineate mechanisms underlying their expansion and contribution in the onset and progression of the pulmonary blood vessel remodeling.

PCs differ in origin, morphology, and function, depending on the organ and vascular bed studied. In lungs of tamoxifen injected *NG2CreER<sup>TM</sup>;mT/mG* mice, they are irregularly distributed through the lung parenchyma and exhibit long cytoplasmic processes, a characteristic supporting their strong capacity to establish contact with numerous cells and thus integrate signals along the length of the blood vessel. However, PCs located on the precapillary vessels ( $> 70\mu\text{m}$ ) lose these extensions and tend to wrap around the vessel. On precapillary vessels, PCs are more frequently  $\alpha$ -SMA-positive relative to PCs located in the parenchymal lung tissue (**Figure 2B** and **S4**). Even if their expressions are not exclusive to this cell-type, pulmonary PCs are known to express the cell surface 3G5 ganglioside antigen, the chondroitin sulfate proteoglycan NG2, and PDGF receptor- $\beta$ <sup>7, 24-29</sup>. To test if pulmonary PCs are phenotypically and functionally altered in PAH, control and PAH PCs were isolated using an anti-3G5 antibody and anti-IgM magnetic beads and studied at very early passages ( $\leq 4$ ). These primary human cultures were  $> 95\%$  pure and expressed typical PC markers such as CD73, CD90, CD105, c-kit, nestin, RGS5, S100 calcium-binding A4 (S100A4), and vimentin. We also find that cultured PAH PCs have greater migration and proliferation potentials than control PCs. Our results are consistent with the fact that a small proportion of PCs ( $\sim 5$  to  $10\%$ ) are positive for proliferating cell nuclear antigen (PCNA) in lungs of PAH patients<sup>7</sup>. In addition, PCs purified from lungs of patients with idiopathic PAH display greater myogenic potentials than control PCs when they are serum deprived. Together, these results argue the existence of intrinsic abnormalities in PAH PCs that influence their cell behavior even when they are extracted from their pathological environment. Consistent with this notion, a recent transcriptome analysis of lung PCs revealed up-regulation in *Fzd7* and *cdc42*, two members involved in the Wnt/ planar cell polarity pathway that is responsible for coordinating complex cell movements during tissue morphogenesis<sup>24</sup>. This notion is also supported by the fact that Wnt5a and endothelium-PC interactions are progressively lost in distal vessels in PAH<sup>25</sup>.

We have provided multiple lines of evidence showing a dynamic role of PCs in the pulmonary blood vessel remodeling *in vivo*. In the present fate-mapping study performed with tamoxifen injected *NG2CreER<sup>TM</sup>;mT/mG* mice chronically exposed to hypoxia, we find an early expansion of NG2<sup>+</sup> cells in mouse lungs that can serve locally as a potential source of  $\alpha$ SMA<sup>+</sup> cells to muscularize distal pulmonary arterioles. Even if the resident PA-SMCs represent the main cellular sources during the pulmonary vascular remodeling associated to PAH<sup>22</sup>, pulmonary PCs orchestrate multiple critical functions that can also indirectly contribute to this process, especially through their connections with the endothelium. As suggested by previous works<sup>7, 22, 23, 30</sup>, we cannot also exclude the contribution of other perivascular progenitors and the presence of several subpopulations of pulmonary PCs. This notion may explain some inconsistencies or contradictory findings in the literature<sup>22-25, 27</sup>. Herein we identified a central role of CXCL12 in PC accumulation within the pulmonary vascular wall. We demonstrate that daily treatments of tamoxifen injected *NG2CreER<sup>TM</sup>;mT/mG* mice with CXCL12 neutraligand chalcone 4 started 2 days before exposure to hypoxia can partially prevent the early increase in pulmonary NG2<sup>+</sup> cells when compared with vehicle treated mice. Our results are consistent with the fact that CXCL12 neutralization or inhibition with the conventional CXCR4 blockade with AMD3100 is beneficial against the pulmonary blood vessel remodeling in preclinical model of pulmonary hypertension, including the SU5416 combined with hypoxia (SuHx) rat model<sup>18, 31</sup>. In lungs of patients with idiopathic PAH a stronger immunoreactivity for CXCL12, CXCR4 and CXCR7 has been reported<sup>18, 32-35</sup>. In the present study, we find that PCs overexpress CXCR7 in lungs from patients with iPAH, a phenomenon that contribute to their pro-proliferative and pro-migratory phenotype. This altered phenotype can facilitate their accumulation around pulmonary blood vessels in PAH through the recruitment of PCs from lost pulmonary blood vessels. Further experiments using transgenic animals are needed to delineate mechanisms underlying these CXCR7 up-regulation observed in PAH and to precise the role of CXCL12/CXCR4/CXCR7

chemotactic axis in the homing and retention of different bone marrow–derived or tissue-resident progenitor cells that could potentially give rise to PCs.

The PDGF and TGF- $\beta$  signaling systems are two additional central molecular regulators in PC biology. Genetic ablations of PDGF-B or PDGF-R $\beta$  in mice is also known to cause severe reduction or even total loss of PCs, and subsequently results in excessive dilation of blood vessels, which causes edema formation and embryonic lethality<sup>36-41</sup>. We have previously demonstrated that TGF- $\beta$ , that is over-activated in lungs of PAH patients, is a strong inducer of PC differentiation into smooth muscle-like cells *in vitro*<sup>7</sup>. Consistent with these findings, we analyzed the ability of PAH PCs to respond to TGF $\beta$  and they elicited a greater induction of Smad2/3 phosphorylation,  $\alpha$ -SMA and SM22 than control PCs. Analysis of relative protein levels of TGF receptors revealed that this greater myogenic potential was partly explained by the TGF $\beta$ RII up-regulation. Interestingly, mice knockout (KO) for TGF $\beta$ RII die during early embryogenesis with profound defects in vasculature and PC/smooth muscle cell induction and differentiation<sup>42</sup>. Consistent with this notion, inhibition of TGF- $\beta$  signaling<sup>43,44</sup> or disruption of its signaling by expression of an inducible dominant negative mutation of the TGF $\beta$ RII<sup>45</sup> attenuate the pulmonary blood vessel remodeling and pulmonary hypertension in rodents. These observations suggest that the beneficial effect of TGF- $\beta$  inhibition on pulmonary vascular remodeling in experimental PH models could be partly explained by a reduction in pericyte accumulation around pulmonary vessels. Since conditional deletion of *Tgfb2* in hematopoietic cells interferes with the differentiation of myeloid progenitors into PCs in the embryonic skin<sup>46</sup>, it would be interesting to know whether myeloid progenitors overexpress or not TGF $\beta$ RII in PAH. Finally, it is known that other pathways including the signaling through the Rho GTPase pathway or Notch3 are central for PC behaviors and thus may also contribute to the processes of microvascular stabilization, maturation, and contractility during PAH development<sup>47,48</sup>.

Based on our lineage tracing and functional studies, we have provided definitive evidence that pulmonary PCs are mobilized under certain conditions to muscularize distal pulmonary blood vessels (**Figure 7**). The demonstration that pulmonary PCs are altered in patients with idiopathic PAH and overexpress CXCR7 and TGF $\beta$ RII has relevance to our understanding of the pathophysiological blood vessel remodeling occurring in lungs of patients with PAH. This knowledge may have major ramifications for the research and development of innovative therapeutic strategies.

## **Acknowledgments:**

The authors thank Maria-Rosa Ghigna, Caroline Communaux and all technicians and pathologists from the Department of Pathology at Marie Lannelongue hospital for their expertise and support. The authors thank Valérie Domergue and her team from the animal facility of UMS IPSIT for their help with the animals. The authors also thank Valérie Drouet and Fabienne Regnier from the Institut Cochin photonic imaging facility (IMAG'IC) for their help with the preparation of the Human precision-cut lung slices. The authors thank Dominique Bonnet, Nelly Frossard and their teams from the "Laboratoire d'Innovation Thérapeutique", UMR7200 CNRS, Université de Strasbourg and LabEx MEDALIS for providing chalcone 4.

## **Sources of Funding:**

This research was supported by grants from the French National Institute for Health and Medical Research (INSERM), the University of Paris-Sud and the Université Paris-Saclay, the Marie Lannelongue Hospital, the French National Agency for Research (ANR) grant no. ANR-16-CE17-0014 (TAMIRAH) and ANR-15-CE14-0020 (PAHVAP), the Fondation pour la Recherche Médicale (FRM) grant no. DEQ20150331712 (Equipe FRM 2015) and in part by the Département Hospitalo-Universitaire (DHU) Thorax Innovation (TORINO), the Assistance Publique-Hôpitaux de Paris (AP-HP), Service de Pneumologie, Centre de Référence de l'Hypertension Pulmonaire Sévère, the LabEx LERMIT (grant no ANR-10-LABX-0033), the French PAH patient association (HTAP France) and the french Fonds de Dotation "Recherche en Santé Respiratoire" - (FRSR) - Fondation du Souffle (FdS). This research was also supported in part by an investigator-sponsored study (ISS) grant from GlaxoSmithKline (GSK). J.B. is supported by the FRM. N.B. is supported The Ile-de-France Regional Council with a doctoral contract (ARDoC 2018).

## **Disclosures:**

J.B., L.T, N.B., R.T., A.C., B.L.V., E.F., S.N., A.H, and C.G. have no conflict of interest to disclose. In the past 3 years, M.H. and L.S. report grants, personal fees, and nonfinancial support from Actelion, Bayer, GlaxoSmithKline, and MSD, outside of the submitted work. M.H. is a member of the Scientific Advisory Board of Morphogen-IX.

## References:

1. Simonneau G, Montani D, Celermajer DS, Denton CP, Gatzoulis MA, Krowka M, Williams PG, Souza R. Haemodynamic definitions and updated clinical classification of pulmonary hypertension. *Eur Respir J.* 2019;53
2. Humbert M, Guignabert C, Bonnet S, Dorfmuller P, Klinger JR, Nicolls MR, Olschewski AJ, Pullamsetti SS, Schermuly RT, Stenmark KR, Rabinovitch M. Pathology and pathobiology of pulmonary hypertension: State of the art and research perspectives. *Eur Respir J.* 2019;53
3. Armulik A, Genove G, Betsholtz C. Pericytes: Developmental, physiological, and pathological perspectives, problems, and promises. *Dev Cell.* 2011;21:193-215
4. Armulik A, Abramsson A, Betsholtz C. Endothelial/pericyte interactions. *Circ Res.* 2005;97:512-523
5. Payne LB, Zhao H, James CC, Darden J, McGuire D, Taylor S, Smyth JW, Chappell JC. The pericyte microenvironment during vascular development. *Microcirculation.* 2019
6. Stallcup WB. The ng2 proteoglycan in pericyte biology. *Adv Exp Med Biol.* 2018;1109:5-19
7. Ricard N, Tu L, Le Hiress M, Huertas A, Phan C, Thuillet R, Sattler C, Fadel E, Seferian A, Montani D, Dorfmuller P, Humbert M, Guignabert C. Increased pericyte coverage mediated by endothelial-derived fibroblast growth factor-2 and interleukin-6 is a source of smooth muscle-like cells in pulmonary hypertension. *Circulation.* 2014;129:1586-1597
8. Guignabert C, Alvira CM, Alastalo TP, Sawada H, Hansmann G, Zhao M, Wang L, El-Bizri N, Rabinovitch M. Tie2-mediated loss of peroxisome proliferator-activated receptor-gamma in mice causes pdgf receptor-beta-dependent pulmonary arterial muscularization. *Am J Physiol Lung Cell Mol Physiol.* 2009;297:L1082-1090
9. Tamura Y, Phan C, Tu L, Le Hiress M, Thuillet R, Jutant EM, Fadel E, Savale L, Huertas A, Humbert M, Guignabert C. Ectopic upregulation of membrane-bound il6r drives vascular remodeling in pulmonary arterial hypertension. *J Clin Invest.* 2018;128:1956-1970
10. Tu L, Desroches-Castan A, Mallet C, Guyon L, Cumont A, Phan C, Robert F, Thuillet R, Bordenave J, Sekine A, Huertas A, Ritvos O, Savale L, Feige JJ, Humbert M, Bailly S, Guignabert C. Selective bmp-9 inhibition partially protects against experimental pulmonary hypertension. *Circ Res.* 2019;124:846-855
11. Huertas A, Tu L, Thuillet R, Le Hiress M, Phan C, Ricard N, Nadaud S, Fadel E, Humbert M, Guignabert C. Leptin signalling system as a target for pulmonary arterial hypertension therapy. *Eur Respir J.* 2015;45:1066-1080
12. Le Hiress M, Tu L, Ricard N, Phan C, Thuillet R, Fadel E, Dorfmuller P, Montani D, de Man F, Humbert M, Huertas A, Guignabert C. Proinflammatory signature of the dysfunctional endothelium in pulmonary hypertension. Role of the macrophage migration inhibitory factor/cd74 complex. *Am J Respir Crit Care Med.* 2015;192:983-997
13. Tu L, De Man FS, Girerd B, Huertas A, Chaumais MC, Lecerf F, Francois C, Perros F, Dorfmuller P, Fadel E, Montani D, Eddahibi S, Humbert M, Guignabert C. A critical role for p130cas in the progression of pulmonary hypertension in humans and rodents. *Am J Respir Crit Care Med.* 2012;186:666-676
14. Tu L, Dewachter L, Gore B, Fadel E, Dartevielle P, Simonneau G, Humbert M, Eddahibi S, Guignabert C. Autocrine fibroblast growth factor-2 signaling contributes to altered endothelial phenotype in pulmonary hypertension. *Am J Respir Cell Mol Biol.* 2011;45:311-322
15. Manders E, Verbeek F, Aten JA. *Measurement of colocalization of objects in dual-color confocal images.* 1993.
16. Ciuculan L, Bonneau O, Hussey M, Duggan N, Holmes AM, Good R, Stringer R, Jones P, Morrell NW, Jarai G, Walker C, Westwick J, Thomas M. A novel murine model of severe pulmonary arterial hypertension. *Am J Respir Crit Care Med.* 2011;184:1171-1182
17. Kucia M, Reza R, Miekus K, Wanzeck J, Wojakowski W, Janowska-Wieczorek A, Ratajczak J, Ratajczak MZ. Trafficking of normal stem cells and metastasis of cancer stem cells involve similar mechanisms: Pivotal role of the sdf-1-cxcr4 axis. *Stem Cells.* 2005;23:879-894
18. Bordenave J, Thuillet R, Tu L, Phan C, Cumont A, Marsol C, Huertas A, Savale L, Hibert M, Galzi JL, Bonnet D, Humbert M, Frossard N, Guignabert C. Neutralization of cxcl12 attenuates established pulmonary hypertension in rats. *Cardiovasc Res.* 2019

19. Hachet-Haas M, Balabanian K, Rohmer F, Pons F, Franchet C, Lecat S, Chow KY, Dagher R, Gizzi P, Didier B, Lagane B, Kellenberger E, Bonnet D, Baleux F, Haiech J, Parmentier M, Frossard N, Arenzana-Seisdedos F, Hibert M, Galzi JL. Small neutralizing molecules to inhibit actions of the chemokine cxcl12. *J Biol Chem*. 2008;283:23189-23199
20. Regenass P, Abboud D, Daubeuf F, Lehalle C, Gizzi P, Riche S, Hachet-Haas M, Rohmer F, Gasparik V, Boeglin D, Haiech J, Knehans T, Rognan D, Heissler D, Marsol C, Villa P, Galzi JL, Hibert M, Frossard N, Bonnet D. Discovery of a locally and orally active cxcl12 neutraligand (lit-927) with anti-inflammatory effect in a murine model of allergic airway hypereosinophilia. *J Med Chem*. 2018;61:7671-7686
21. Ding R, Darland DC, Parmacek MS, D'Amore PA. Endothelial-mesenchymal interactions in vitro reveal molecular mechanisms of smooth muscle/pericyte differentiation. *Stem Cells Dev*. 2004;13:509-520
22. Sheikh AQ, Saddouk FZ, Ntokou A, Mazurek R, Greif DM. Cell autonomous and non-cell autonomous regulation of smc progenitors in pulmonary hypertension. *Cell Rep*. 2018;23:1152-1165
23. Crnkovic S, Marsh LM, El Agha E, Voswinckel R, Ghanim B, Klepetko W, Stacher-Priehse E, Olschewski H, Bloch W, Bellusci S, Olschewski A, Kwapiszewska G. Resident cell lineages are preserved in pulmonary vascular remodeling. *J Pathol*. 2018;244:485-498
24. Yuan K, Orcholski ME, Panaroni C, Shuffle EM, Huang NF, Jiang X, Tian W, Vladar EK, Wang L, Nicolls MR, Wu JY, de Jesus Perez VA. Activation of the wnt/planar cell polarity pathway is required for pericyte recruitment during pulmonary angiogenesis. *Am J Pathol*. 2015;185:69-84
25. Yuan K, Shamskhov EA, Orcholski ME, Nathan A, Reddy S, Honda H, Mani V, Zeng Y, Ozen MO, Wang L, Demirci U, Tian W, Nicolls MR, de Jesus Perez VA. Loss of endothelium-derived wnt5a is associated with reduced pericyte recruitment and small vessel loss in pulmonary arterial hypertension. *Circulation*. 2019;139:1710-1724
26. Yuan K, Orcholski ME, Huang NF, de Jesus Perez VA. In vivo study of human endothelial-pericyte interaction using the matrix gel plug assay in mouse. *J Vis Exp*. 2016
27. Yuan K, Shao NY, Hennigs JK, Discipulo M, Orcholski ME, Shamskhov E, Richter A, Hu X, Wu JC, de Jesus Perez VA. Increased pyruvate dehydrogenase kinase 4 expression in lung pericytes is associated with reduced endothelial-pericyte interactions and small vessel loss in pulmonary arterial hypertension. *Am J Pathol*. 2016;186:2500-2514
28. Chang YT, Tseng CN, Tannenberg P, Eriksson L, Yuan K, de Jesus Perez VA, Lundberg J, Lengquist M, Botusan IR, Catrina SB, Tran PK, Hedin U, Tran-Lundmark K. Perlecan heparan sulfate deficiency impairs pulmonary vascular development and attenuates hypoxic pulmonary hypertension. *Cardiovasc Res*. 2015;107:20-31
29. Stallcup WB. The ng2 proteoglycan: Past insights and future prospects. *J Neurocytol*. 2002;31:423-435
30. Dierick F, Hery T, Hoareau-Coudert B, Mougnot N, Monceau V, Claude C, Crisan M, Besson V, Dorfmueller P, Marodon G, Fadel E, Humbert M, Yaniz-Galende E, Hulot JS, Marazzi G, Sassoon D, Soubrier F, Nadaud S. Resident pw1+ progenitor cells participate in vascular remodeling during pulmonary arterial hypertension. *Circ Res*. 2016;118:822-833
31. Farkas D, Kraskauskas D, Drake JI, Alhussaini AA, Kraskauskiene V, Bogaard HJ, Cool CD, Voelkel NF, Farkas L. Cxcr4 inhibition ameliorates severe obliterative pulmonary hypertension and accumulation of c-kit(+) cells in rats. *PLoS One*. 2014;9:e89810
32. Costello CM, McCullagh B, Howell K, Sands M, Belperio JA, Keane MP, Gaine S, McLoughlin P. A role for the cxcl12 receptor, cxcr7, in the pathogenesis of human pulmonary vascular disease. *Eur Respir J*. 2012;39:1415-1424
33. Farha S, Asosingh K, Xu W, Sharp J, George D, Comhair S, Park M, Tang WH, Loyd JE, Theil K, Tubbs R, Hsi E, Lichtin A, Erzurum SC. Hypoxia-inducible factors in human pulmonary arterial hypertension: A link to the intrinsic myeloid abnormalities. *Blood*. 2011;117:3485-3493
34. Gambaryan N, Perros F, Montani D, Cohen-Kaminsky S, Mazmanian M, Renaud JF, Simonneau G, Lombet A, Humbert M. Targeting of c-kit+ haematopoietic progenitor cells prevents hypoxic pulmonary hypertension. *Eur Respir J*. 2011;37:1392-1399

35. McCullagh BN, Costello CM, Li L, O'Connell C, Codd M, Lawrie A, Morton A, Kiely DG, Condliffe R, Elliot C, McLoughlin P, Gaine S. Elevated plasma cxcl12alpha is associated with a poorer prognosis in pulmonary arterial hypertension. *PLoS One*. 2015;10:e0123709
36. Hellstrom M, Kalen M, Lindahl P, Abramsson A, Betsholtz C. Role of pdgf-b and pdgfr-beta in recruitment of vascular smooth muscle cells and pericytes during embryonic blood vessel formation in the mouse. *Development*. 1999;126:3047-3055
37. Leveen P, Pekny M, Gebre-Medhin S, Swolin B, Larsson E, Betsholtz C. Mice deficient for pdgf b show renal, cardiovascular, and hematological abnormalities. *Genes Dev*. 1994;8:1875-1887
38. Lindahl P, Johansson BR, Leveen P, Betsholtz C. Pericyte loss and microaneurysm formation in pdgf-b-deficient mice. *Science*. 1997;277:242-245
39. Soriano P. Abnormal kidney development and hematological disorders in pdgf beta-receptor mutant mice. *Genes Dev*. 1994;8:1888-1896
40. Enge M, Bjarnegard M, Gerhardt H, Gustafsson E, Kalen M, Asker N, Hammes HP, Shani M, Fassler R, Betsholtz C. Endothelium-specific platelet-derived growth factor-b ablation mimics diabetic retinopathy. *EMBO J*. 2002;21:4307-4316
41. Lebrin F, Srun S, Raymond K, Martin S, van den Brink S, Freitas C, Breant C, Mathivet T, Larrivee B, Thomas JL, Arthur HM, Westermann CJ, Disch F, Mager JJ, Snijder RJ, Eichmann A, Mummery CL. Thalidomide stimulates vessel maturation and reduces epistaxis in individuals with hereditary hemorrhagic telangiectasia. *Nat Med*. 2010;16:420-428
42. Oshima M, Oshima H, Taketo MM. Tgf-beta receptor type ii deficiency results in defects of yolk sac hematopoiesis and vasculogenesis. *Dev Biol*. 1996;179:297-302
43. Poble PB, Phan C, Quatremare T, Bordenave J, Thuillet R, Cumont A, Huertas A, Tu L, Dorfmuller P, Humbert M, Ghigna MR, Savale L, Guignabert C. Therapeutic effect of pirfenidone in the sugen/hypoxia rat model of severe pulmonary hypertension. *FASEB J*. 2019;33:3670-3679
44. Yung LM, Nikolic I, Paskin-Flerlage SD, Pearsall RS, Kumar R, Yu PB. A selective transforming growth factor-beta ligand trap attenuates pulmonary hypertension. *Am J Respir Crit Care Med*. 2016;194:1140-1151
45. Chen YF, Feng JA, Li P, Xing D, Zhang Y, Serra R, Ambalavanan N, Majid-Hassan E, Oparil S. Dominant negative mutation of the tgf-beta receptor blocks hypoxia-induced pulmonary vascular remodeling. *J Appl Physiol (1985)*. 2006;100:564-571
46. Yamazaki T, Nalbandian A, Uchida Y, Li W, Arnold TD, Kubota Y, Yamamoto S, Ema M, Mukoyama YS. Tissue myeloid progenitors differentiate into pericytes through tgf-beta signaling in developing skin vasculature. *Cell Rep*. 2017;18:2991-3004
47. Ji Y, Chen S, Xiang B, Li Y, Li L, Wang Q. Jagged1/notch3 signaling modulates hemangioma-derived pericyte proliferation and maturation. *Cell Physiol Biochem*. 2016;40:895-907
48. Kutcher ME, Kolyada AY, Surks HK, Herman IM. Pericyte rho gtpase mediates both pericyte contractile phenotype and capillary endothelial growth state. *Am J Pathol*. 2007;171:693-701

## FIGURE LEGENDS

### Figure 1. Characterization of pulmonary pericytes

(A) Experimental procedure to isolate pulmonary pericytes (PCs) and their characterization by multi-color flow cytometry. Blues curves are obtained with specific antibodies against the antigen and red curves are results obtained with non-relevant antibodies. We labeled samples in duplicate, using non-immune isotype-specific antibodies for one aliquot (red curve) and specific antibodies for the other (blue curve). The non-immune fluorescence gave the background for the sample.

(B) Immunofluorescence staining of NG2 (green), PDGFR- $\beta$  (green),  $\alpha$ -SMA (green), calponin (red), SMMHC (red) and DAPI (blue) in cultured pulmonary pericytes

(C-D) Comparison of surface markers between human pulmonary PCs and human pulmonary artery smooth muscle cells (PA-SMCs) and human pulmonary artery adventitial fibroblasts (PAAFs) in primary cultures using RT-qPCR: The isolated PCs did not express characteristic smooth muscle or fibroblast markers.

(E) Expression of gene characteristics of human pulmonary mesenchymal stem cells (HPMSCs) using RT-qPCR.

Data are presented as mean  $\pm$  SEM; \* p-value < 0.05; \*\* p-value < 0.01; \*\*\* p-value < 0.001; \*\*\*\* p-value < 0.0001 *versus* PA-SMCs, PAAFs or HMSCs. Scale bar = 50  $\mu$ m in all sections

### Figure 2. Pulmonary pericytes are altered in Human PAH

(A) Scratch-wound closure monitored over time in primary cultures of pulmonary pericytes from control (n = 6) and idiopathic PAH patients (n = 5). Representative bright-field images and quantification of the wound closure expressed as the remaining area uncovered by the cells.

(B) Representative images of stained cells attached to the lower surface of polycarbonate membranes. Quantitative analysis of the number of cells migrated through a polycarbonate membrane during six hours (n = 6-7).

(C) Basal proliferative potential of pulmonary pericytes from control (n = 7) and idiopathic PAH patients (n = 7) was assessed by BrdU incorporation.

(D) Representative Western blot and quantification of the SM22:GAPDH, calponin: $\beta$ -actin,  $\alpha$ -SMA:GAPDH and Col1A:GAPDH ratios in pulmonary pericytes from control (n = 7) and iPAH patients (n = 8) in the complete medium or after serum deprivation (48 h).

Data are presented as mean  $\pm$  SEM; \* p-value < 0.05; \*\* p-value < 0.01; \*\*\* p-value < 0.001 *versus* control cells ## p-value < 0.01 *versus* control cells under serum deprivation. Scale bar = 50  $\mu$ m in all sections. AU = arbitrary unit.

### Figure 3. Pericytes dynamically contribute to the blood vessel remodeling in hypoxia-induced distal pulmonary arteriole muscularization

(A) Experimental scheme to lineage trace NG2-expressing cells *in vivo* under hypoxia for 2, 4, 7, 14, or 21 days or kept in room air.

(B) Lung vibratome sections from a tamoxifen injected *NG2CreER<sup>TM</sup>;mT/mG* stained maintained in room air for GFP (green),  $\alpha$ -SMA (red) and MECA (grey) (n = 5).

(C) Lung vibratome sections of normoxic or hypoxic *NG2CreER<sup>TM</sup>;mT/mG* mice injected with tamoxifen and stained for GFP (green),  $\alpha$ -SMA (red) and MECA (grey). Quantification of GFP positive cells and of  $\alpha$ -SMA positive cells expressing GFP (10 vessels per mouse; n=3 animals per condition).

(D) FACS plot and percentage of cells double positive for GFP and  $\alpha$ -SMA in lungs from tamoxifen injected *NG2CreER<sup>TM</sup>;mT/mG* mice maintained in room air (n = 14) or chronically exposed to hypoxia for 7 (n = 8), 14 (n = 8), or 21 days (n=12). Flow cytometry gating conditions were set against isotype- and fluorophore-matched non-immune IgGs.

Data are presented as mean  $\pm$  SEM; \* p-value < 0.05; \*\* p-value < 0.01; \*\*\*\* p-value < 0.0001 *versus* normoxia # p-value < 0.05 *versus* D2; \$\$ p-value < 0.01; \$\$\$ p-value < 0.001 *versus* D4. Scale bar = 50  $\mu$ m in all sections. AU = arbitrary unit.

**Figure 4. Pericytes differentiate into contractile cells to muscularize distal arterioles in mice subjected to SU5416 followed by 3-week hypoxia to induce severe PH**

- (A) Experimental scheme to lineage trace NG2-expressing cells *in vivo* in tamoxifen injected *NG2CreER<sup>TM</sup>;mT/mG* mice treated or not with SU5416 and chronically exposed to hypoxia for 3 weeks
- (B) Lung vibratome sections of tamoxifen injected *NG2CreER<sup>TM</sup>;mT/mG* mice maintained in room air (n = 3) or treated with SU5416 and chronically exposed to hypoxia (n = 3) stained for GFP (green),  $\alpha$ -SMA (red) and MECA (grey). Quantification of GFP positive cells and of  $\alpha$ -SMA positive cells expressing GFP.
- (C) FACS plot and percentage of cells double positive for GFP and  $\alpha$ -SMA in lungs from tamoxifen injected *NG2CreER<sup>TM</sup>;mT/mG* mice maintained in room air (n = 5) or treated with SU5416 and chronically exposed to hypoxia (n = 8). Flow cytometry gating conditions were set against isotype- and fluorophore-matched non-immune IgGs.
- Data are presented as mean  $\pm$  SEM; \* p-value < 0.05; \*\*\*\* p-value < 0.0001 *versus* normoxic mice. Scale bar = 50  $\mu$ m in all sections. AU = arbitrary unit.

**Figure 5. CXCL12 is required for the early pericyte accumulation in lungs of mice chronically exposed to hypoxia**

- (A) Gene expression analysis of CXCL12 mRNA levels in mouse lungs under hypoxia for 2, 4, 7, 14, or 21 days or kept in room air.
- (B) Scheme of Chalcone 4 administration of *NG2CreER<sup>TM</sup>;mT/mG* mice, prior to exposure to hypoxia for 2 or 4 days.
- (C) Lung vibratome sections of tamoxifen injected *NG2CreER<sup>TM</sup>;mT/mG* mice maintained in hypoxia and treated with either vehicle (n = 3) or chalcone 4 (n = 3) stained for GFP (green),  $\alpha$ -SMA (red) and MECA (grey).
- (D) FACS plot and percentage of GFP positive cells from tamoxifen injected *NG2CreER<sup>TM</sup>;mT/mG* mice maintained in room air (n = 9) or chronically exposed to hypoxia in presence of vehicle (n = 8-10) or Chalcone 4 (n = 6-7). Flow cytometry gating conditions were set against isotype- and fluorophore-matched non-immune IgGs. Percentage of GFP positive cells is shown.
- (E) Representative Western blot and quantification of the GFP: $\beta$ -actin and NG2: $\beta$ -actin ratios in lungs of tamoxifen injected *NG2CreER<sup>TM</sup>;mT/mG* mice maintained in room air (n = 12-13) or chronically exposed to hypoxia in presence of vehicle (n = 11-14) or Chalcone 4 (n = 7-14). Data are presented as mean  $\pm$  SEM; \* p-value < 0.05; \*\* p-value < 0.01; \*\*\* p-value < 0.001; \*\*\*\* p-value < 0.0001 *versus* normoxic mice. # p-value < 0.05; ## p-value < 0.01; ##### p-value < 0.0001 *versus* hypoxic mice treated with vehicle. Scale bar = 50  $\mu$ m in all sections. AU = arbitrary unit.

**Figure 6. CXCR7 is up-regulated in pulmonary pericytes of patients with idiopathic PAH**

- (A) Proliferation of pulmonary pericytes from control (n = 8) and idiopathic PAH patients (n = 8) induced by CXCL12 at the indicated doses was assessed by BrdU incorporation.
- (B) Representative images of stained cells attached to the lower surface of polycarbonate membranes. Quantitative analysis of the number of cells migrated through a polycarbonate membrane during six hours in response to 100ng/mL of CXCL12 (n = 7-8).
- (C) Representative Western blot and quantification of the CXCR4: $\beta$ -actin and CXCR7: $\beta$ -actin ratios in pulmonary pericytes from control (n = 7-8) and idiopathic PAH patients (n = 7-8)
- (D) Confocal immunofluorescence analyses of CXCR7, 3G5 and DAPI in paraffin sections of pulmonary arterioles from human controls (n = 4) and idiopathic PAH patients (n = 4). Bottom panels show a higher magnification of 3G5 positive cells.
- (E) Representative images of pulmonary pericytes derived from patients with idiopathic PAH attached to the lower surface of polycarbonate membranes. Quantitative analysis of the number of cells migrated through a polycarbonate membrane during six hours in response to 1% FCS in presence of AMD3100, Chalcone 4, or vehicle at the indicated doses (n = 4-5).
- (F) Proliferation of pulmonary pericytes derived from patients with idiopathic PAH (n = 5) in response to 1% FCS in presence of AMD3100, Chalcone 4, or vehicle at the indicated doses.

**(G)** Representative images of idiopathic pulmonary pericytes attached to the lower surface of polycarbonate membranes. Quantitative analysis of the number of cells migrated through a polycarbonate membrane during six hours in presence of 5 nM of VUF 11207 (n = 5).

**(H)** Proliferation of pulmonary pericytes derived from patients with idiopathic PAH (n = 5) in presence of 5 nM of VUF 11207 (n = 5).

Data are presented as mean  $\pm$  SEM; \* p-value < 0.05; \*\* p-value < 0.01; \*\*\* p-value < 0.001; \*\*\*\* p-value < 0.0001 *versus* the appropriate control condition. ## p-value < 0.01; ### p-value < 0.001; ##### p-value < 0.0001 *versus* vehicle. Scale bar = 50  $\mu$ m in all sections. AU = arbitrary unit.

**Figure 7. TGF $\beta$ RII overexpression in Human PAH pericytes increased their susceptibility to respond to TGF $\beta$  -induced differentiation**

**(A)** Representative Western blot and quantification of the  $\alpha$ -SMA: $\beta$ -actin, SM22: $\beta$ -actin ratios in pulmonary pericytes from control (n = 5) and patients with idiopathic PAH (n = 8) exposed to 10ng/mL of TGF- $\beta$ .

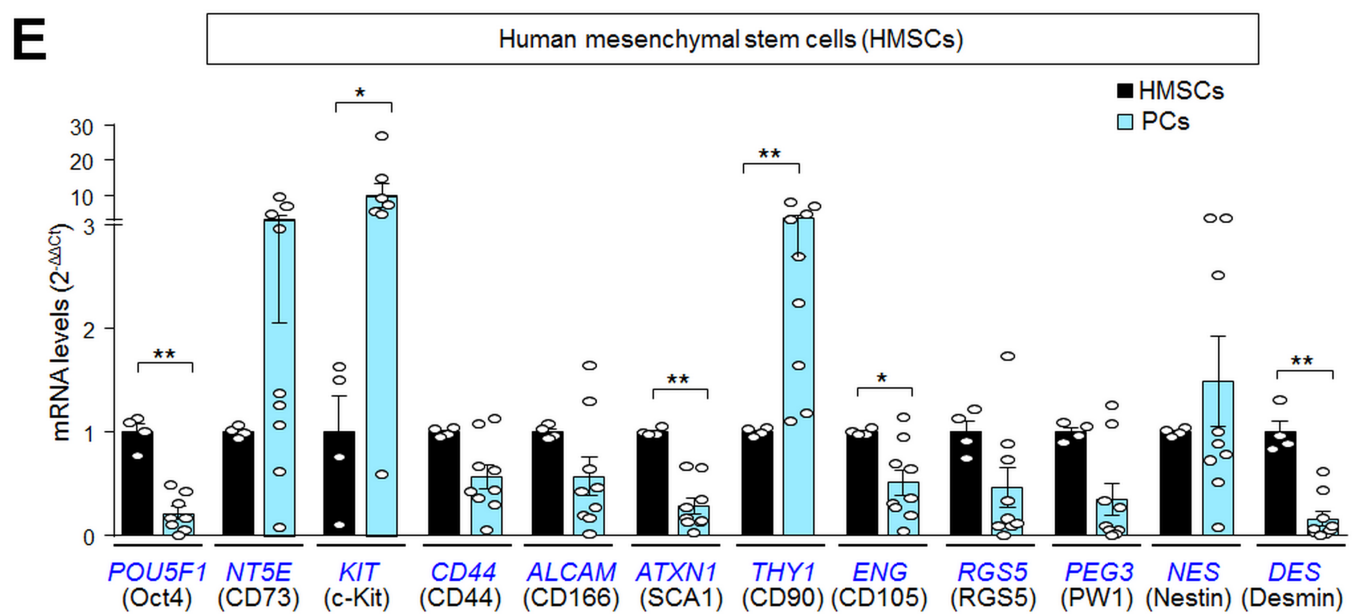
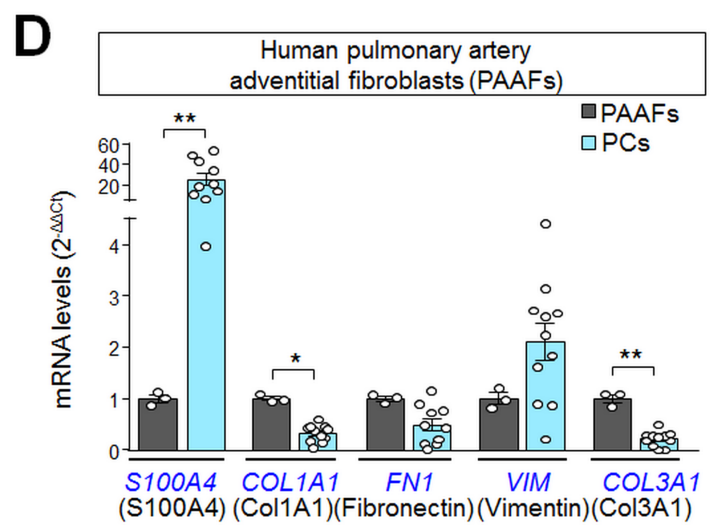
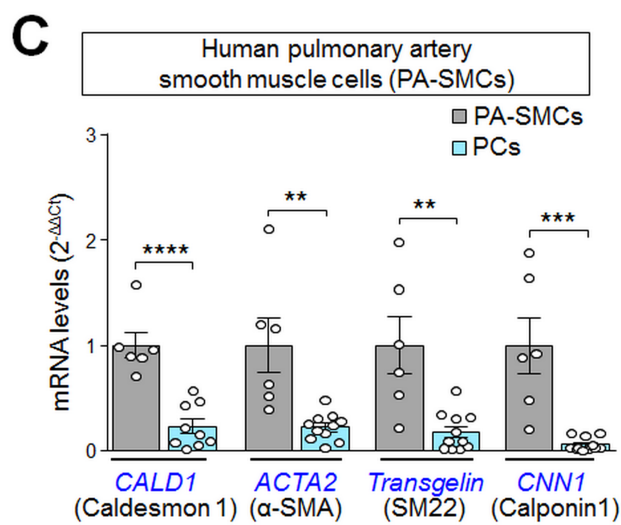
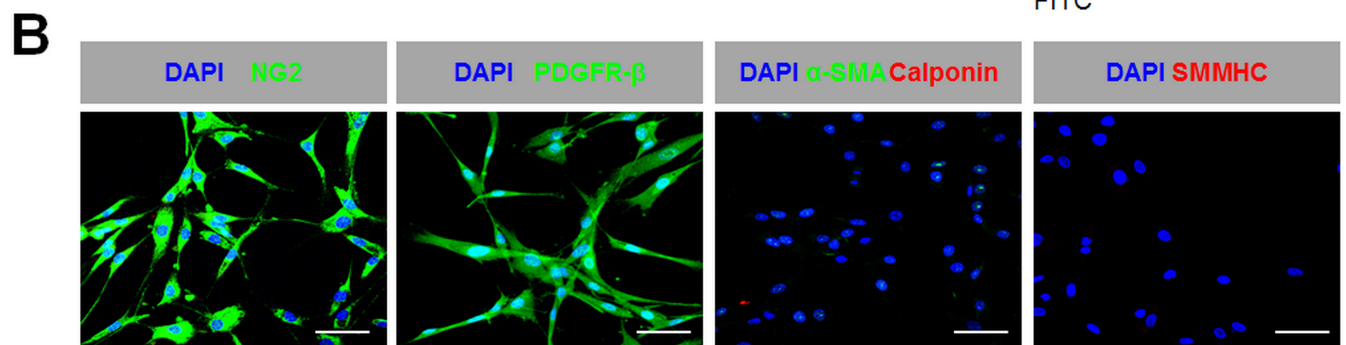
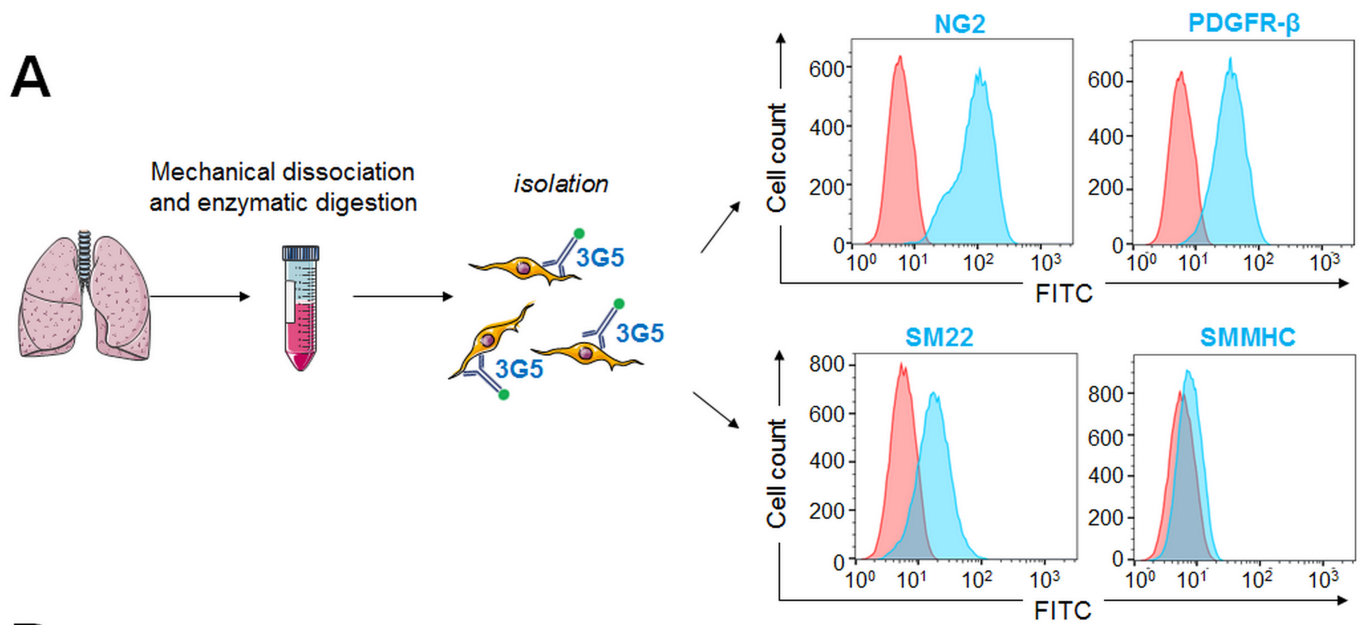
**(B)** Representative Western blot and quantification of the p-smad2/3: $\beta$ -actin ratio in pulmonary pericytes from control (n = 5-7) and patients with idiopathic PAH (n = 5) exposed to 10ng/mL of TGF- $\beta$  at different times.

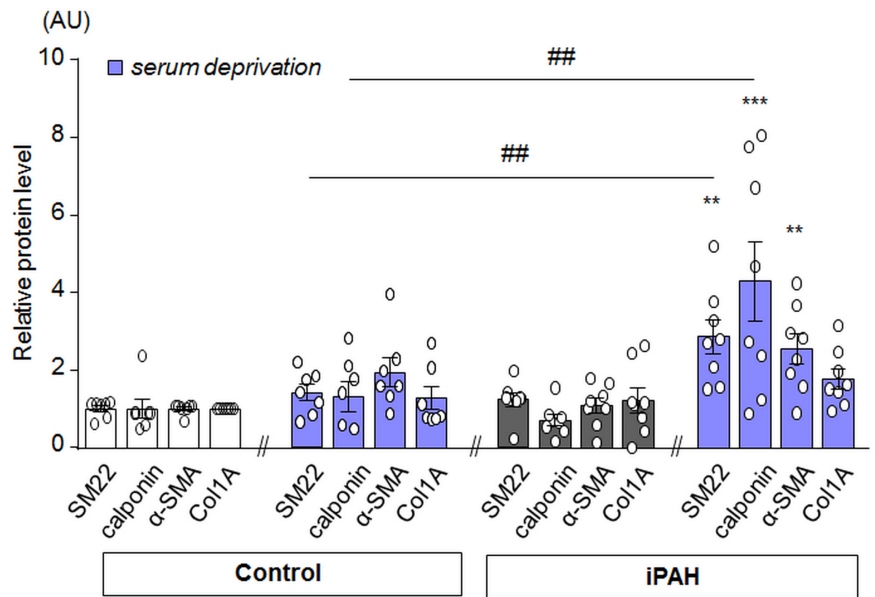
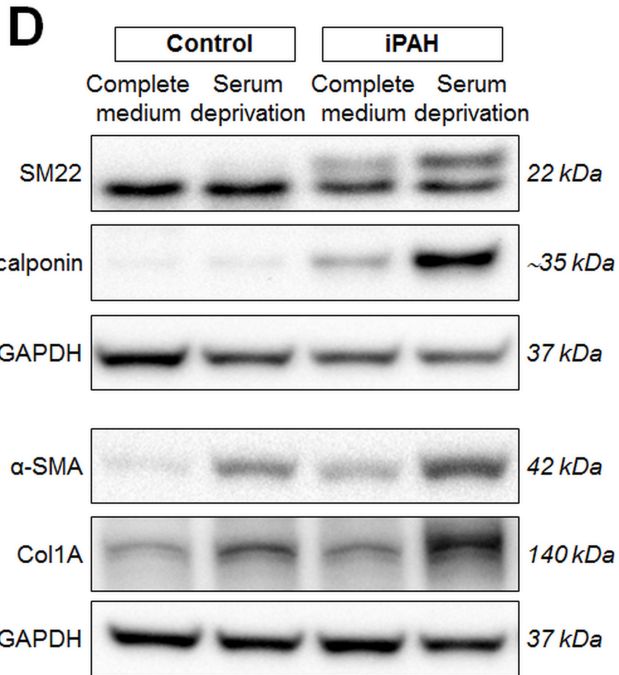
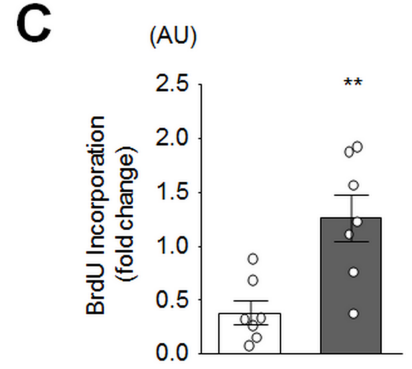
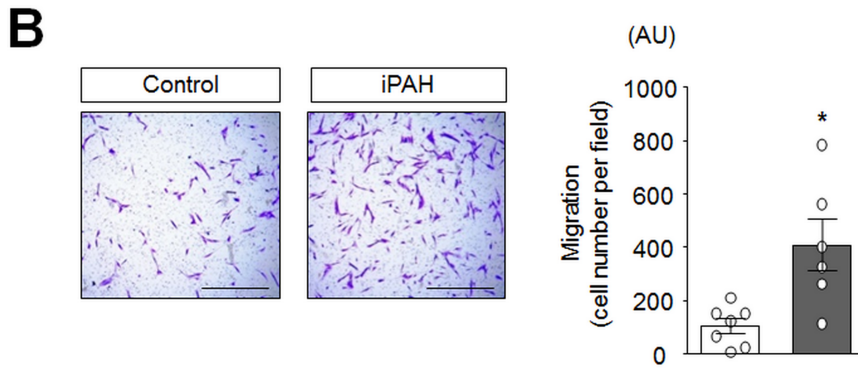
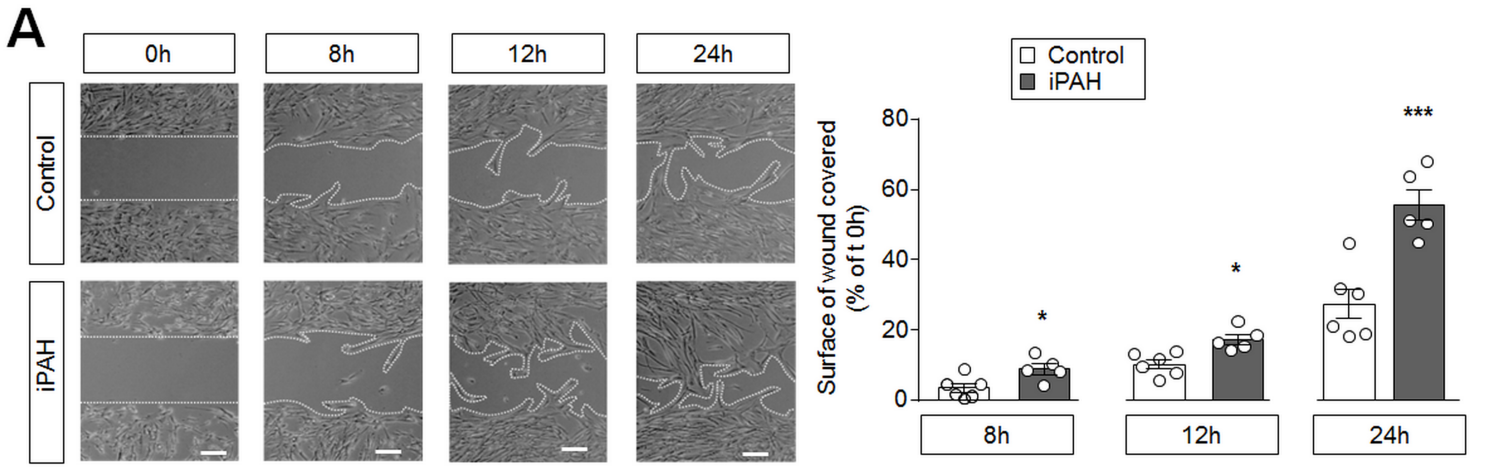
**(C)** Representative Western blot and quantification of the TGF $\beta$ RII:GAPDH, and TGF $\beta$ RI:GAPDH ratios in pulmonary pericytes from control (n = 8-10) and patients with idiopathic PAH (n = 9).

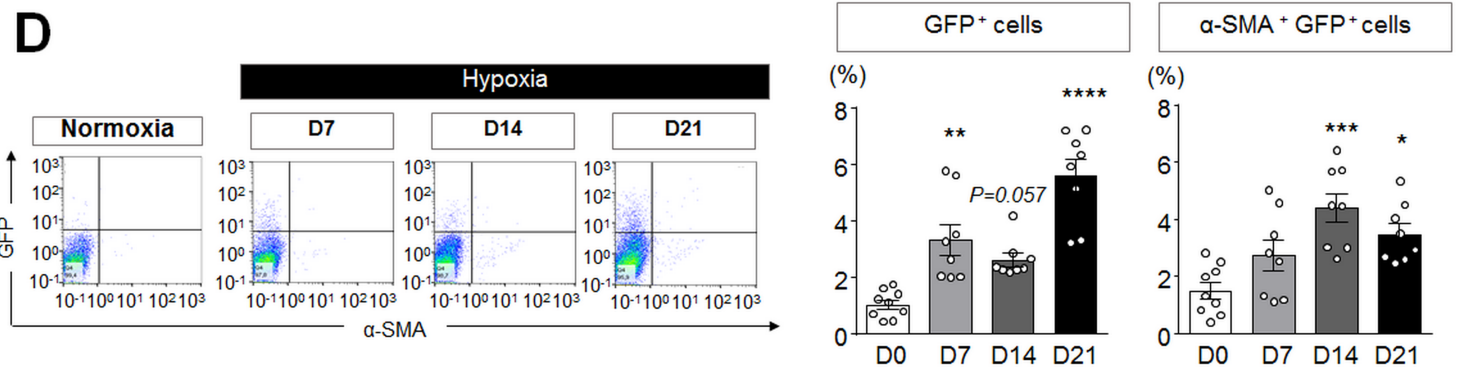
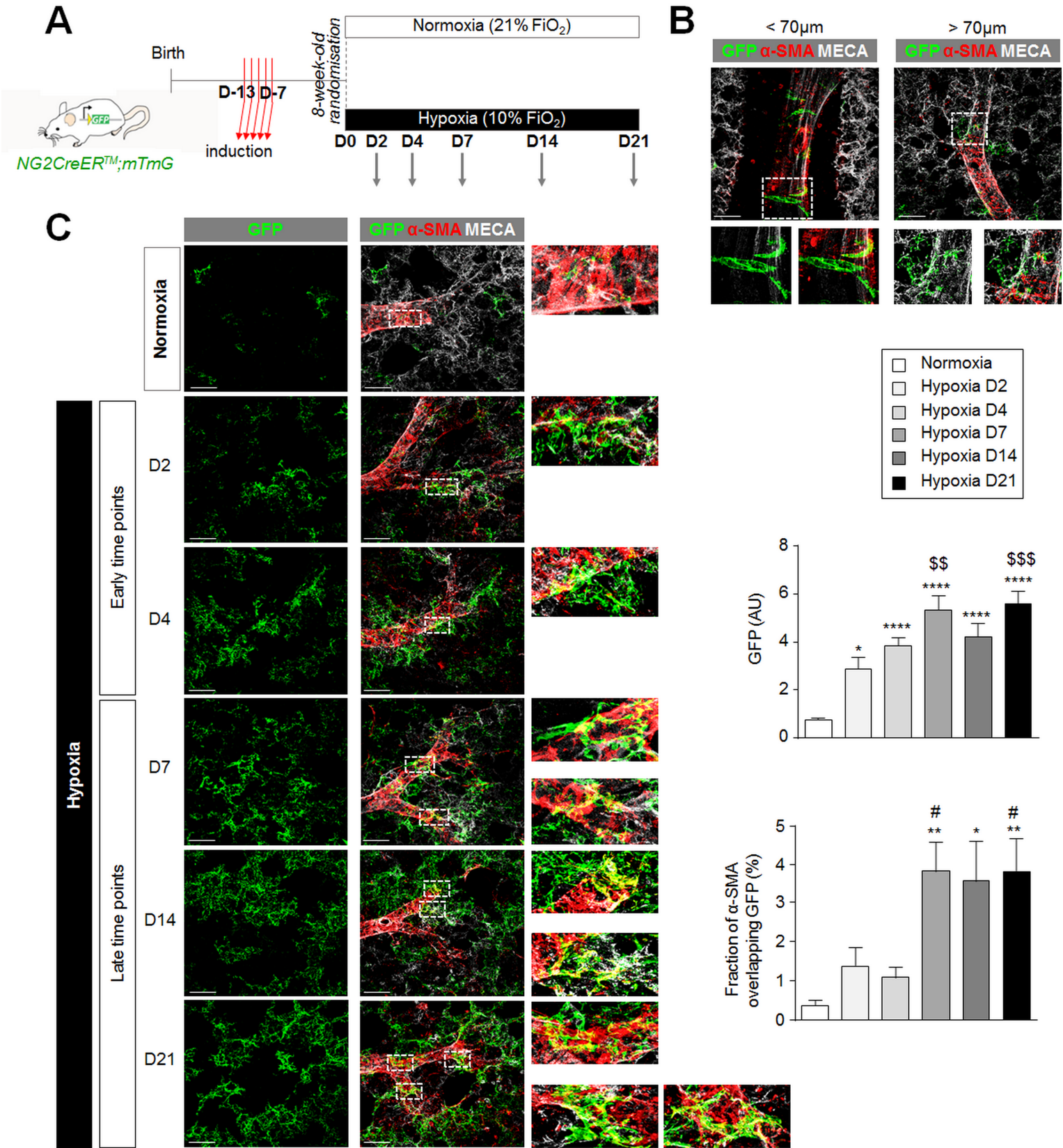
**(D)** Confocal immunofluorescence analyses of TGF $\beta$ RII, 3G5,  $\alpha$ -SMA, and DAPI in paraffin sections of pulmonary arterioles from human controls (n = 3) and idiopathic PAH patients (n = 3). Right panels show a higher magnification of 3G5 positive cells.

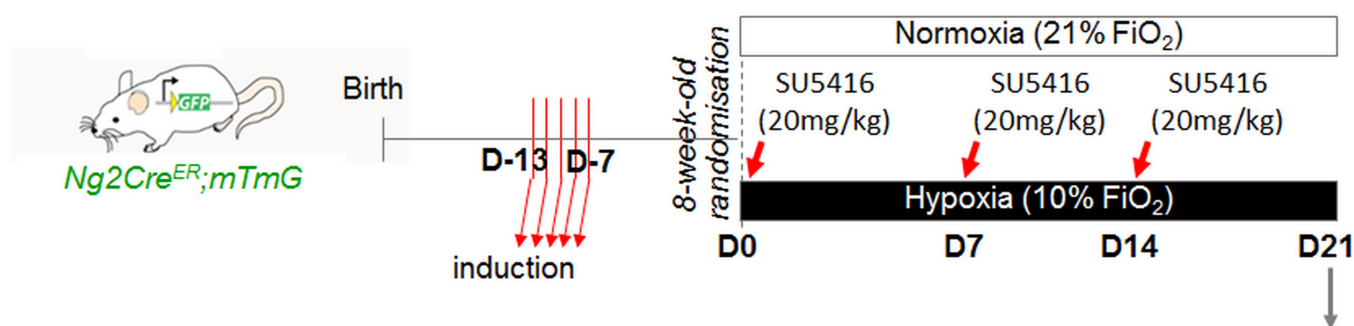
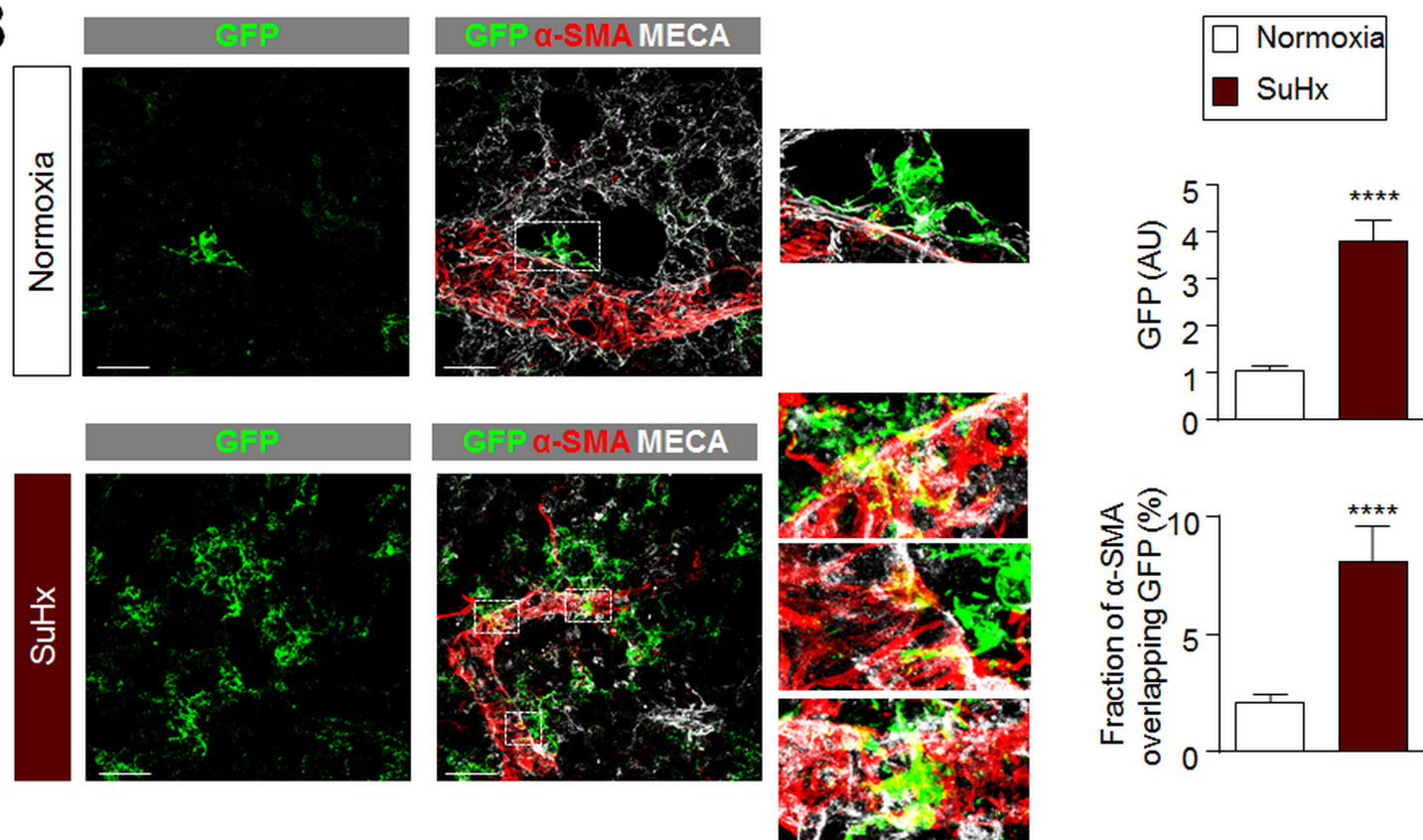
Data are presented as mean  $\pm$  SEM; \* p-value < 0.05; \*\* p-value < 0.01; \*\*\*\* p-value < 0.0001 *versus* control pericytes or t0. # p-value < 0.05; ## p-value < 0.01 *versus* control pericytes. Scale bar = 50  $\mu$ m in all sections. AU = arbitrary unit.

**Figure 8. Dynamic role of pericytes in the pulmonary blood vessel remodeling in PAH**







**A****B****C**